

Heat/Mass Driven Natural Convection Of Air Near A Boundary Of Constant Mass Flux And Temperature

Maria Neagu

Manufacturing Engineering Department
"Dunarea de Jos" University of Galati,
Galati, Romania
Maria.Neagu@ugal.ro

Abstract—This paper is an analysis of the natural convection process that occurs near a vertical boundary of a constant temperature and of constant mass flux of a certain constituent, a boundary that is embedded in a mass stratified and constant temperature environment. Throughout the paper the environment considered is air, the Lewis number and the Smith number are greater than 1.0. The successions of the heat and/or the mass driven convection processes that attain the equilibrium state along the wall are revealed using the scale analysis method, while the finite differences method is used to verify these results for two particular cases. This analysis concludes that, depending on the process parameters, only two situations can be encountered: a heat driven convection regime or a succession of heat and mass driven convection regimes along the boundary.

Keywords—*natural convection; mass stratification; constant mass flux; scale analysis; finite differences method*

I. INTRODUCTION

This paper belongs to a group of research analyses [1-4] of the natural convection process along a vertical impermeable wall embedded in a porous or a fluid medium saturated with a certain constituent such that the environment is thermally and/or mass stratified. Using the scale analysis method, these analyses prove that a heat and/or a mass driven natural convection succession attains the equilibrium state along the wall, a succession that depends on the process characteristics and parameters. All these studies [1-4] conclude that a specific coefficient defines the heat and/or the mass driven convection regimes succession along the vertical boundary.

This paper analyzes the case of a vertical impermeable wall situated in a $Pr < 1$ environment (air, $Pr = 0.72$) saturated with a certain constituent such that the Lewis number $Le \geq 1$ and the Smith number $Sch \geq 1$ (see Fig. 1). The temperature of the wall is constant (T_w), while a constant mass flux (m_w) of the constituent is registered at the wall. Far from the wall, the environment registers a constant temperature (T_∞) and a linearly varying concentration of the constituent, $C_{\infty,x}$.

The scale analysis indicates the existence of a heat driven convection (HDC) regime or a HDC-MDC (mass driven convection) regime succession according to Fig. 2. The finite differences solution of the governing equations verifies the scale analysis results for two parameter sets.

II. MATHEMATICAL FORMULATION

Fig. 1 presents the wall and the Cartesian coordinate system attached to it, as well as the boundary conditions. The concentration of the constituent is: $C_{\infty,x} = C_{\infty,0} + s_c \cdot x$, as $x \rightarrow \infty$, where s_c is the environment stratification parameter. In the case of a fluid whose density obeys the Boussinesq approximation, the governing equations become [2]:

$$\frac{\partial v}{\partial x} + \frac{\partial u}{\partial y} = 0; \quad (1)$$

$$\frac{\partial u}{\partial t} + u \cdot \frac{\partial u}{\partial y} + v \cdot \frac{\partial u}{\partial x} = -\frac{\partial p}{\partial y} + \nu \left(\frac{\partial^2 u}{\partial x^2} + \frac{\partial^2 u}{\partial y^2} \right); \quad (2)$$

$$\frac{\partial v}{\partial t} + u \cdot \frac{\partial v}{\partial y} + v \cdot \frac{\partial v}{\partial x} = -\frac{\partial p}{\partial x} + \nu \left(\frac{\partial^2 v}{\partial x^2} + \frac{\partial^2 v}{\partial y^2} \right) + g\beta_t T + g\beta_c C; \quad (3)$$

$$\frac{\partial T}{\partial t} + u \cdot \frac{\partial T}{\partial y} + v \cdot \frac{\partial T}{\partial x} = \alpha \left(\frac{\partial^2 T}{\partial x^2} + \frac{\partial^2 T}{\partial y^2} \right); \quad (4)$$

$$\frac{\partial C}{\partial t} + u \cdot \frac{\partial C}{\partial y} + v \cdot \frac{\partial C}{\partial x} + v \cdot s_c = D \left(\frac{\partial^2 C}{\partial x^2} + \frac{\partial^2 C}{\partial y^2} \right). \quad (5)$$

The boundary conditions are [2]:

$$u = v = 0, T = T_w, \frac{\partial C}{\partial y} = -\Gamma_w \text{ at } y = 0; \quad (6)$$

$$v = 0, T = T_\infty, C = C_{\infty,x} \text{ as } y \rightarrow \infty; \quad (7)$$

$$v = 0, T = T_\infty, C = C_{\infty,0} \text{ at } x = 0; \quad (8)$$

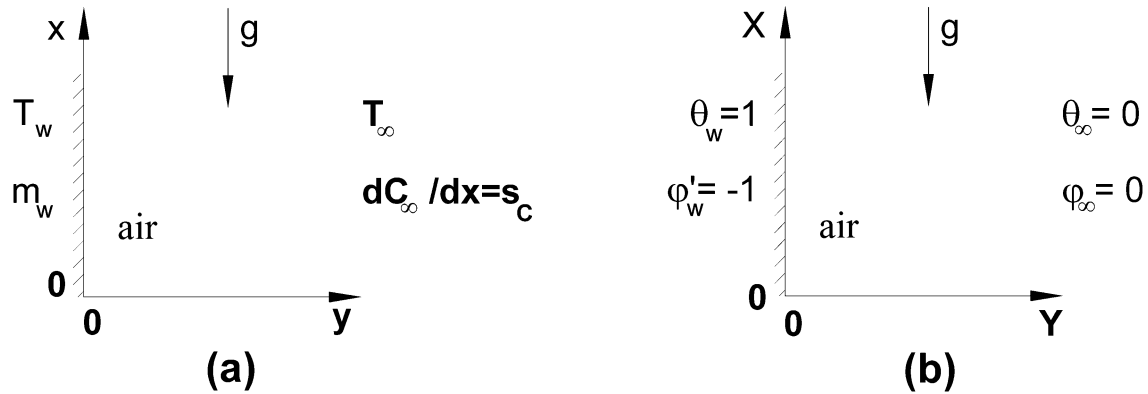


Fig. 1. (a) The dimensional problem; (b) the dimensionless problem.

$$\frac{\partial^2 u}{\partial x^2} = \frac{\partial^2 v}{\partial x^2} = \frac{\partial^2 T}{\partial x^2} = \frac{\partial^2 C}{\partial x^2} = 0 \text{ at } x = h, \quad (9)$$

where: t is the time, T the temperature, C the concentration, h the upper limit of the computational domain, u/v the horizontal and the vertical velocity, respectively, while p is the environment pressure, α thermal diffusivity, D mass diffusivity, ν kinematic viscosity. $\Gamma_w = m_w/D$ is the concentration gradient at the boundary, β_c and β_t are the coefficients of volumetric expansion with concentration and temperature, respectively.

III. SCALE ANALYSIS

This section studies the transient state (A), the equilibrium heat driven convection (HDC) regime (B) and the equilibrium mass driven convection (MDC) regime (C) using the scale analysis method [5].

A. Scale Analysis of the Transient State

During the transient state, the equilibrium between the inertia and the horizontal diffusion of heat (equation (4)) or the horizontal diffusion of the species (equation (5)) defines the boundary layer thickness of the temperature field [2]:

$$\delta_T \sim \alpha^{1/2} \cdot t^{1/2} \quad (10)$$

or of the concentration field [2]:

$$\delta_C \sim D^{1/2} \cdot t^{1/2}. \quad (11)$$

The study realised by [2] defines two aspects of interest for this analysis:

- at the beginning, a HDC regime occurs at each abscissa along the wall and it is replaced by a MDC regime only if the equilibrium time at that abscissa is bigger than the transition time, t_{trz} [2]:

$$t_{trz} \sim L^2 \cdot (N^2 D)^{-1}, \quad (12)$$

where N is the buoyancy ratio: $N = \beta_c \Gamma_w L / \beta_t$ and L is the reference length;

- at the beginning, the $v \cdot s_c$ term is the dominant term on the left side of equation (5), but the $v \cdot \partial C / \partial x$ term could become greater than the $v \cdot s_c$ term if the equilibrium time at that abscissa is greater than t_s [2].

$$t_s \sim \frac{s_c^2 x^2}{\Gamma_w^2 D}. \quad (13)$$

B. Scale Analysis of the Heat Driven Convection Regime

As a HDC regime is registered at each abscissa along the wall during the first moments of the transition state, this HDC regime will be analysed first. Section 3.3 will analyse the MDC regime.

For $Pr < 1$, $Le \geq 1$ case, [6] proves that the vertical velocity order of magnitude is:

$$v_T \sim \frac{g \beta_t t}{1 + Pr} \Delta T, \quad (14)$$

while the velocity boundary layer thickness is $\delta_v = (Pr)^{1/2} \delta_T$ and the Prandtl number is $Pr = \nu / \alpha$. Requiring the equilibrium between the horizontal diffusion and the vertical convection of heat [2], the temperature equilibrium time, boundary layer thickness and vertical velocity magnitudes are discovered:

$$(t_{ech,T})_T \sim \left[\frac{x(1 + Pr)}{g \beta_t} \right]^{1/2} = \frac{L^2}{\alpha} \left[\frac{X(1 + Pr)}{Ra \cdot Pr} \right]^{1/2} \quad (15)$$

$$(\delta_{ech,T})_T \sim L \cdot \left[\frac{X(1 + Pr)}{Ra \cdot Pr} \right]^{1/4}; \quad (16)$$

$$V_T \sim \left(\frac{X \cdot Ra \cdot Pr}{1 + Pr} \right)^{1/2}, \quad (17)$$

where $X = x/L$, $V = vL/\alpha$, $Ra = g \beta_t L^3 / (\alpha \nu)$.

Scale analysis of the concentration field in the HDC regime: the concentration field for the

Sch = v/D = Le · Pr ≥ 1 case is characterized by the vertical velocity $(v_C)_T = v_T \cdot \delta_C / \delta_V$. We note that Le = α/D.

Two situations appear:

1) If $v \cdot \partial C / \partial x$ is the dominant term in the left side of equation (5): The equilibrium between the horizontal diffusion of the constituent and the vertical convection of it determines the equilibrium time and boundary layer thickness of the concentration field:

$$(t_{ech,C})_T \sim \frac{L^2}{D} \left[\frac{X(1+Pr)Pr}{Ra} \right]^{1/2} \frac{1}{Sch^{2/3}}; \quad (18)$$

$$(\delta_{ech,C})_T \sim L \left[\frac{X(1+Pr)Pr}{Ra} \right]^{1/4} \frac{1}{Sch^{1/3}}. \quad (19)$$

The dimensionless vertical velocity order of magnitude of the concentration field in the HDC regime becomes: $(V_C)_T = X / Sch^{1/3}$.

The equilibrium time of the concentration field, $(t_{ech,C})_T$, is bigger than the transition time, $t_{tr,z}$:

$$X > X_{tr,z,C} = Ra \cdot Pr^{1/3} \cdot Le^{4/3} \cdot N^{-4} / (1+Pr). \quad (20)$$

2) If the $v \cdot s_C$ term is the dominant term in equation (5): Then the equilibrium time and the boundary layer thickness are:

$$(t_{ech,Sc})_T \sim \frac{L^2}{D} \left[\frac{(1+Pr)^3 \cdot Pr^3}{X \cdot Ra^3} \right]^{1/4} \cdot \frac{1}{Sch \cdot S_C}; \quad (21)$$

$$(\delta_{ech,Sc})_T \sim D^{1/2} t^{1/2} = L \left[\frac{(1+Pr)^3 \cdot Pr^3}{X \cdot Ra^3} \right]^{1/8} \cdot \left(\frac{1}{Sch \cdot S_C} \right)^{1/2} \quad (22)$$

, where the dimensionless stratification parameter is $S_C = s_C / \Gamma_w$.

The equilibrium time $(t_{ech,Sc})_T$ is compared to $t_{tr,z}$ and t_s :

a) The equilibrium time $(t_{ech,Sc})_T$ is bigger than the transition time, $t_{tr,z}$, if:

$$X > \frac{N^8}{(S_C \cdot Sch)^4} \left[\frac{Pr(1+Pr)}{Ra} \right]^3 = X_{tr,z,Sc}. \quad (23)$$

b) The inequality $(t_{ech,Sc})_T < t_s$ is restricted to the following domain:

$$X > \left[\frac{1}{S_C^3 \cdot Sch} \right]^{4/9} \left[\frac{Pr(1+Pr)}{Ra} \right]^{1/3} = X_{s,T}. \quad (24)$$

The relative position of these two abscissa, $X_{tr,z,Sc}$ and $X_{s,T}$, along the vertical plane boundary assures the existence of only two possibilities:

- A HDC regime along the wall if $X_{tr,z,Sc} < X_{s,T} < X_{tr,z,C}$ (Fig. 2 (a)) or

$$\frac{Ra \cdot S_C \cdot Sch^{4/3}}{Pr(1+Pr) \cdot N^3} \geq 1. \quad (25)$$

- A HDC regime in the $[0, X_{tr,z,C}]$ domain and a MDC regime in the $[X_{tr,z,Sc}, \infty)$ domain (see Fig. 2 (b)) if $Ra \cdot S_C \cdot Sch^{4/3} / [N^3 Pr(1+Pr)] < 1$.

C. Scale Analysis of the Mass Driven Convection Regime

This analysis has as a point of start the results obtained by [7] and [8]. The equilibrium between viscosity and buoyancy over the entire concentration boundary layer thickness gives us the vertical velocity order of magnitude:

$$v_C \sim g \beta_C \Gamma_w D^{1/2} t^{3/2} A / \nu, \quad (26)$$

where $A = 1$ in [7] and $A = [\sqrt{Sch} / (1 + \sqrt{Sch})]^2$ in [8].

1) MDC_{Sc} regime

In this case, the equilibrium between the horizontal diffusion and the vertical convection of the constituent requires: $v_C \cdot s_C \sim D \left(\frac{\partial^2 C}{\partial y^2} \right)$ or $v_C \cdot s_C \sim D \frac{\Gamma_w}{D^{1/2} t^{1/2}}$.

Replacing v_C from equation (26), the equilibrium time and the boundary layer thickness are:

$$(t_{ech,Sc})_c \sim \frac{L^2}{D} \left[\frac{1}{Ra \cdot N \cdot Le \cdot S_C \cdot A} \right]^{1/2}; \quad (27)$$

$$(\delta_{ech,Sc})_c \sim L [Ra \cdot N \cdot Le \cdot S_C \cdot A]^{-1/4}. \quad (28)$$

At equilibrium, the vertical velocity scales as:

$$V_C \sim [Ra \cdot N \cdot A \cdot Le^{-3} \cdot S_C^{-3}]^{1/4}. \quad (29)$$

The inequality $(t_{ech,Sc})_c < t_s$ or

$$X > [Ra \cdot N \cdot Le \cdot S_C^5 \cdot A]^{-1/4} = X_{s,C} \quad (30)$$

defines the X co-ordinate that separates the MDC_C and the MDC_{Sc} regimes in Fig. 2(b).

Scale analysis of the temperature field in the MDC_{Sc} regime: this analysis requires

$$\left(v_C \frac{\delta_V}{\delta_T} \right) \cdot \frac{\partial T}{\partial x} \sim \alpha \cdot \frac{\partial^2 T}{\partial y^2} \quad \text{or}$$

$$\left(v_C \frac{\sqrt{Sch} \cdot \delta_C}{\delta_T} \right) \cdot \frac{\Delta T}{x} \sim \alpha \frac{\Delta T}{\delta_T^2}. \quad \text{Using the equations (10)}$$

and (29), the temperature boundary layer becomes:

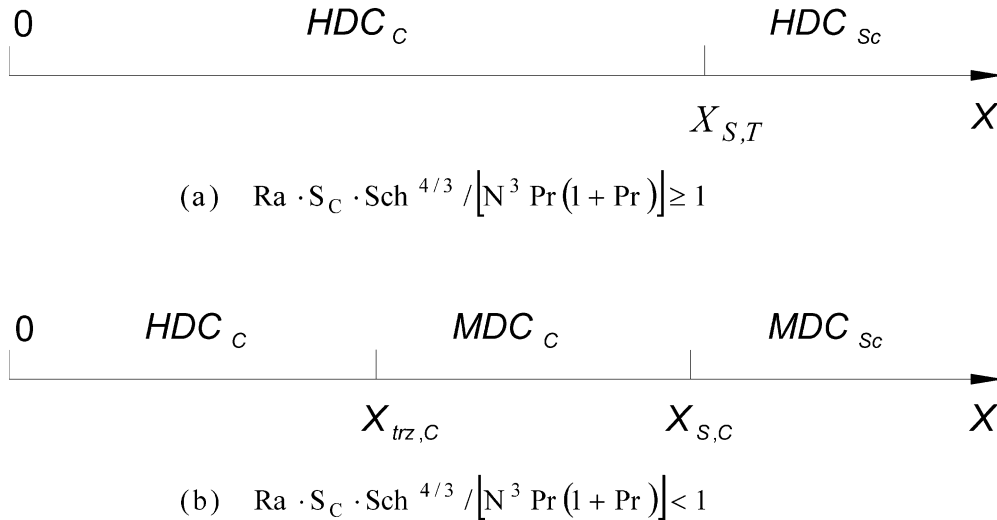


Fig. 2. The heat and mass driven natural convection regimes sequence. (a) $Ra \cdot S_C \cdot Sch^{4/3} / [N^3 Pr(1 + Pr)] \geq 1$; (b) $Ra \cdot S_C \cdot Sch^{4/3} / [N^3 Pr(1 + Pr)] < 1$.

$$(\delta_{ech,T})_{Sc} \sim L \cdot X \cdot Le \cdot S_C / \sqrt{Sch}, \quad (31)$$

while the vertical velocity order of magnitude is $(v_T)_{Sc} \sim Sch / (Le^2 \cdot S_C^{5/4} \cdot X)$.

2) MDC_C regime

The equilibrium between the horizontal diffusion and the vertical convection requires

$$v_C \cdot \frac{\partial C}{\partial x} \sim D \left(\frac{\partial^2 C}{\partial y^2} \right) \text{ or } v_C / x \sim D / \delta_C^2. \text{ Replacing the}$$

equations (11) and (25), the equilibrium time and the concentration boundary layer thickness become:

$$(t_{ech,C})_C \sim \frac{L^2}{D} \left[\frac{X}{Ra \cdot N \cdot Le \cdot A} \right]^{2/5}; \quad (32)$$

$$(\delta_{ech,C})_C \sim L \cdot \left(\frac{X}{Ra \cdot N \cdot Le \cdot A} \right)^{1/5}, \quad (33)$$

while the vertical velocity scales:

$$V_C \sim [Ra \cdot N \cdot A]^{2/5} \cdot (X / Le)^{3/5}. \quad (34)$$

Scale analysis of the temperature field in the MDC_C regime: the equilibrium between the thermal horizontal diffusion and the vertical thermal convection requires

$$v_C \left(\frac{\delta_v}{\delta_T} \right) \cdot \frac{\partial T}{\partial x} \sim \alpha \left(\frac{\partial^2 T}{\partial y^2} \right) \text{ or } v_C \frac{\sqrt{Sch} \delta_C}{\delta_T} \cdot \frac{\Delta T}{x} \sim \alpha \frac{\Delta T}{\delta_T^2}.$$

The temperature boundary layer thickness is:

$$(\delta_{ech,T})_C \sim L \left[\frac{X \cdot Le^4}{Ra \cdot N \cdot A} \right]^{1/5} \cdot \frac{1}{\sqrt{Sch}}. \quad (35)$$

The validity of the scale analysis requires that, at a certain point along the wall, the boundary layer thickness to be smaller than the point abscissas:

- If $C_{Mn} = Ra \cdot S_C \cdot Sch^{4/3} / [N^3 Pr(1 + Pr)] \geq 1$, the inequality $(\delta_{ech,C})_T \ll (\delta_{ech,T})_T$ is always true; the conditions that must be imposed are: $(\delta_{ech,T})_T \ll x$ and $(\delta_{ech,Sc})_T \ll x$ at $X = X_{S,T}$. These two conditions require: $S_C \ll \min(1, C_{Mn} / Pr^{1/3})$.

- If $Ra \cdot S_C \cdot Sch^{4/3} / [N^3 Pr(1 + Pr)] < 1$, the following conditions are required: $(\delta_{ech,T})_T \ll x$ for $X = X_{trz,C}$; $(\delta_{ech,C})_C \ll x$, $(\delta_{ech,T})_C \ll x$, $(\delta_{ech,Sc})_C \ll x$ and $(\delta_{ech,T})_{Sc} \ll x$ for $X = X_{S,C}$. This set of conditions requires: $S_C \ll \min(1, \sqrt{Sch} / Le)$.

Further, the scale analysis results of section III will be verified using the finite differences method for two particular parameters sets.

IV. NUMERICAL MODELING

The stream function formulation of the velocity field:

$$U = -\frac{\partial \Psi}{\partial X} \text{ and } V = \frac{\partial \Psi}{\partial Y}, \text{ and the vorticity definition:}$$

$$\zeta = \frac{\partial V}{\partial Y} - \frac{\partial U}{\partial X}, \text{ define a new dimensionless form of the}$$

governing equations as follows:

$$\zeta = \left(\frac{\partial^2 \Psi}{\partial Y^2} + \frac{\partial^2 \Psi}{\partial X^2} \right); \quad (36)$$

$$\frac{\partial \zeta}{\partial \tau} + U \frac{\partial \zeta}{\partial Y} + V \frac{\partial \zeta}{\partial X} = Pr \cdot \left(\frac{\partial^2 \zeta}{\partial Y^2} + \frac{\partial^2 \zeta}{\partial X^2} \right) + Ra \cdot Pr \cdot \left(\frac{\partial \theta}{\partial Y} + N \frac{\partial \phi}{\partial Y} \right); \quad (37)$$

$$\frac{\partial \theta}{\partial \tau} + U \frac{\partial \theta}{\partial Y} + V \frac{\partial \theta}{\partial X} = \frac{\partial^2 \theta}{\partial Y^2} + \frac{\partial^2 \theta}{\partial X^2}; \quad (38)$$

$$\frac{\partial \phi}{\partial \tau} + U \frac{\partial \phi}{\partial Y} + V \frac{\partial \phi}{\partial X} + VS_C = \frac{I}{Le} \left(\frac{\partial^2 \phi}{\partial Y^2} + \frac{\partial^2 \phi}{\partial X^2} \right) \quad (39)$$

, where $\theta = \frac{T - T_{\infty}}{T_w - T_{\infty}}$, $\phi = \frac{C - C_{\infty,x}}{m_w L \cdot D^{-1}}$, $U = \frac{uL}{\alpha}$ and $\tau = \tau \alpha / L^2$. The boundary conditions become:

$$\Psi = \frac{\partial \Psi}{\partial Y} = 0, \quad \frac{\partial \phi}{\partial Y} = -1, \quad \theta = 1 \quad \text{at } Y = 0; \quad (40)$$

$$\frac{\partial \Psi}{\partial Y} = 0, \quad \zeta = 0, \quad \theta = \phi = 0 \quad \text{as } Y = L; \quad (41)$$

$$\Psi = 0, \quad \zeta = 0, \quad \theta = \phi = 0 \quad \text{at } X = 0; \quad (42)$$

$$\frac{\partial^2 \Psi}{\partial X^2} = \frac{\partial^3 \Psi}{\partial X^3} = \frac{\partial^2 \theta}{\partial X^2} = \frac{\partial^2 \phi}{\partial X^2} = 0 \quad \text{at } X = H. \quad (43)$$

The governing equations, (36)-(39), subjected to the boundary conditions, equations (40)-(43), were solved using the finite differences method, the higher order hybrid scheme [9] using a software created by the author and explained in detail in [2].

The system of equation (36)-(39) were solved using an iterative process: at each time step, equation (36) was solved iteratively till the relative error of Ψ , at each grid point, became less than 10^{-6} . The iterative process stopped when the relative errors of θ , ϕ and ζ , at each grid point, became less than 10^{-6} .

V. RESULTS AND DISCUSSIONS

The software presented above was used to solve the conservation equations for two parameter sets:

$$A. \quad Ra = 5000, \quad N = 1, \\ Le = 2, \quad Pr = 0.72 \quad \text{and} \quad S_C = 0.05$$

This is the $Ra \cdot S_C \cdot Sch^{4/3} / [Pr(1+Pr) \cdot N^3] \geq 1$ case. According to the scale analysis results (Fig. 2(a)), we expect a HDC regime to attain the equilibrium state along the vertical boundary. The HDC_C and the HDC_{S_C} regimes are delimited by the abscissas $X_{S,T} = 2.98$ (equation (24)). A computational dimensionless domain of 0.6×6.0 was discretised uniformly using a 61×301 grid that assures the desired accuracy.

Fig. 3 presents the temperature (Fig. 3(a)), concentration (Fig. 3(b)), stream function (Fig. 3(c)) and $\partial C / \partial X$ (Fig. 3(d)) fields. The concentration field magnitude of Fig. 3(b) never exceeds the value $1/N = 1.0$ which indicates a HDC regime along the entire wall. Fig. 3(d) shows that $\partial c / \partial x > s_c$ or $\partial C / \partial X > 0$ when $X \geq 2.0$.

Fig. 4 chooses and presents the temperature (Fig. 4(a)), concentration (Fig. 4(b)) and vertical velocity (Fig. 4(c)) plots for three sections made at the 1.0; 1.5 and 2.0 abscissa in the HDC_C regime. These plots collapse if the plots variables are scaled using the equations (16), (17) and (19).

Similarly, Fig. 5 presents the temperature (Fig. 5(a)), concentration (Fig. 5(b)) and vertical velocity (Fig. 5(c)) and their scaled versions: Fig. 5(d), Fig. 5(e) and Fig. 5(f), using the equations (16), (17) and (22).

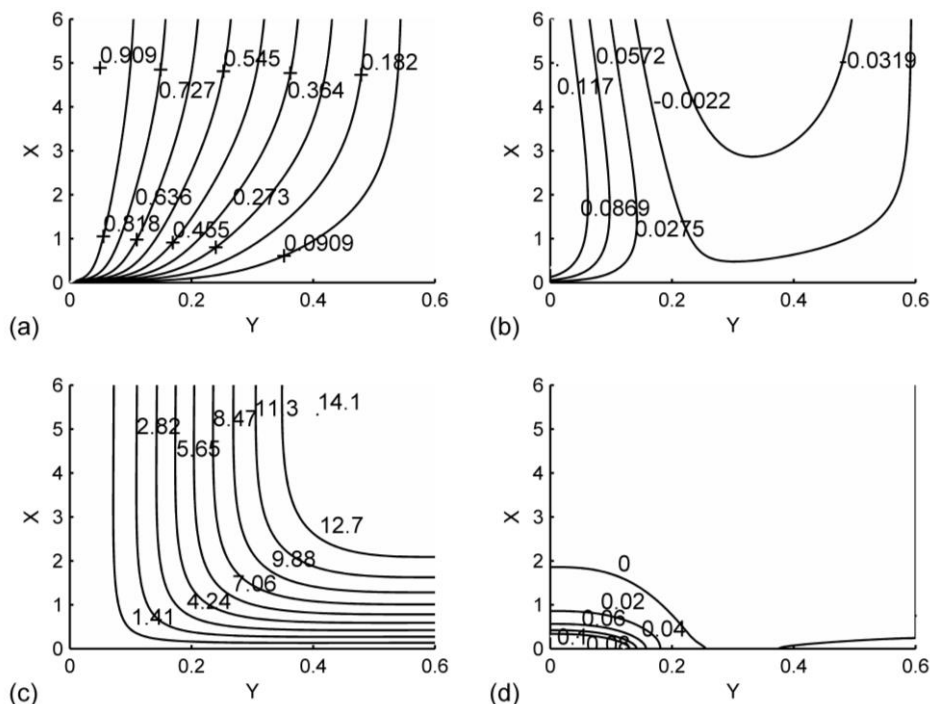


Fig. 3. The dimensionless temperature (a), concentration (b), stream function (c) and $\partial \phi / \partial x$ (d) fields. $Ra = 5000$, $N = 1$, $Le = 2$, $Pr = 0.72$ and $S_C = 0.05$.

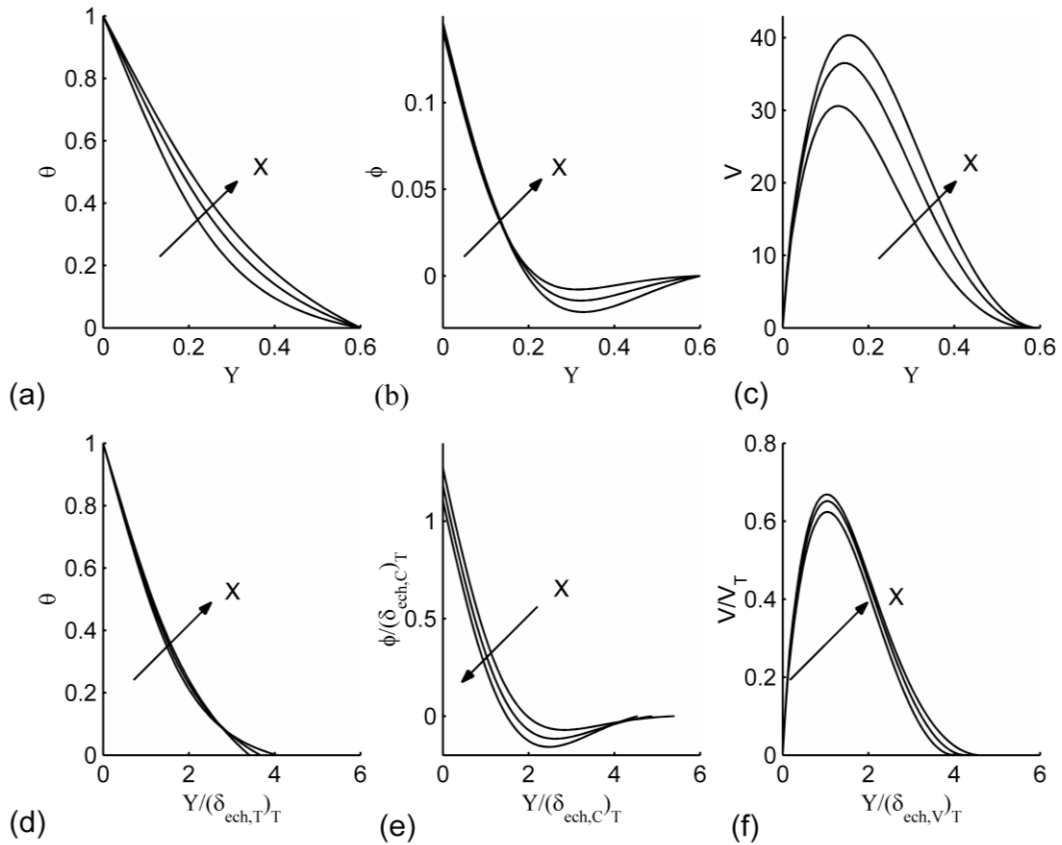


Fig. 5. The dimensionless (a) temperature, (b) concentration and (c) vertical velocity variations as a function of Y and the scaled (d) temperature, (e) concentration and (f) vertical velocity plots for the abscissas: 1.0, 1.5 and 2.0.

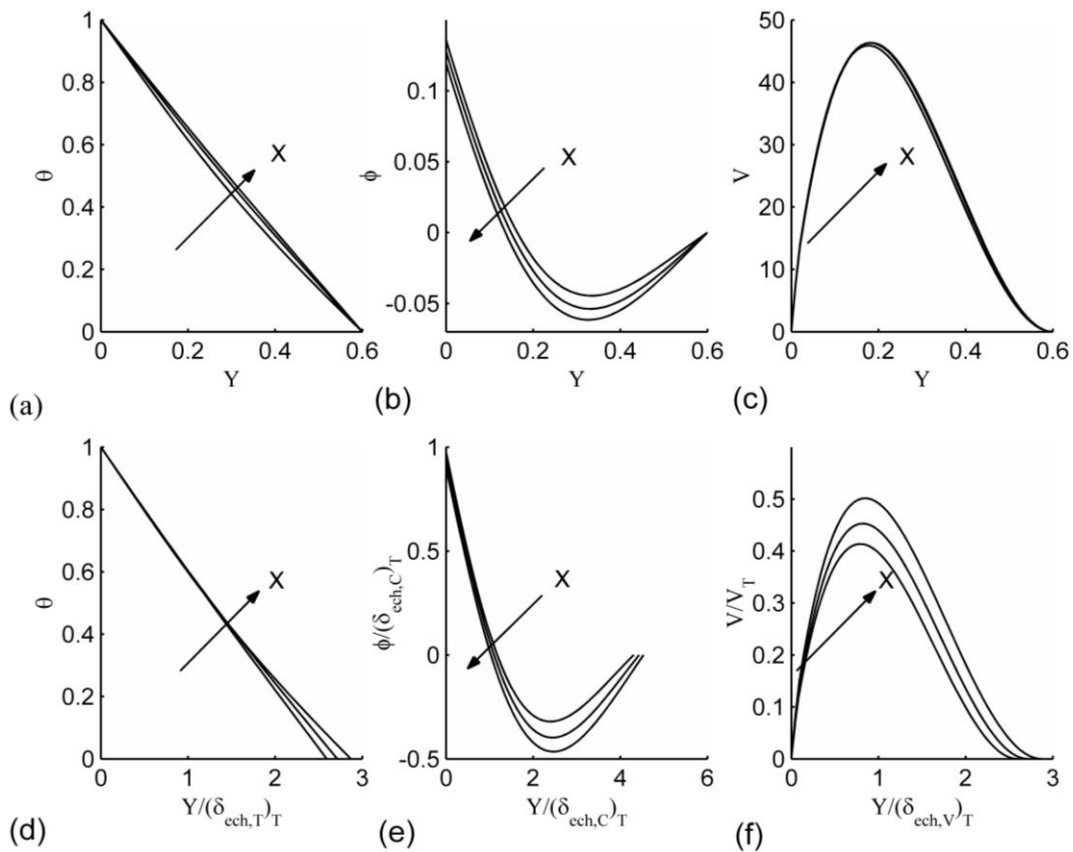


Fig. 4. The dimensionless (a) temperature, (b) concentration and (c) vertical velocity variations as a function of Y and the scaled (d) temperature, (e) concentration and (f) vertical velocity plots for the abscissas: 4.0, 5.0 and 6.0.

The sections were made in the HDC_{Sc} region at the abscissa: 4, 5 and 6.

Fig. 3, Fig. 4 and Fig. 5 prove the validity of the scale analysis results for the $Ra \cdot S_C \cdot Sch^{4/3} / [Pr(1+Pr) \cdot N^3] \geq 1$ case.

B. $Ra = 5000, N = 8,$
 $Le = 2, Pr = 0.72$ and $S_C = 0.04$

The inequality $Ra \cdot S_C \cdot Sch^{4/3} / [Pr(1+Pr) \cdot N^3] < 1$ is valid. A computational dimensionless domain of 0.5×8.0 was discretised uniformly using a 51×401 grid that assures the desired accuracy.

The temperature (Fig. 6(a)), concentration (Fig. 6(b)), stream function (Fig.6(c)) and $\partial C / \partial X$ (Fig. 6(d)) contour plots reveal the following aspects:

- The concentration field at the boundary exceeds $1/N = 1/8$ at $X > 0.62$, a value that is closed to the scale analysis results $X_{trZ} = 1.6$ (equation (20)).
- The $\partial C / \partial X$ field shows that the $\partial c / \partial x > s_c$ or $\partial C / \partial X > 0$ inequality is valid if $X > 5.0$ (equation (30) indicates $X_{Sc} = 4.6$).

Fig. 7, Fig. 8 and Fig. 9 present the plots and the scaled plots for three particular sections along the boundary layer corresponding to the three regime types emphasized above: HDC_C , MDC_C and MDC_{Sc} , as follows:

- Fig. 7 chooses the abscissa 0.2, 0.4 and 0.6 in the HDC_C region. Fig. 7(a), Fig. 7(b) and Fig. 7(c) present the temperature, the concentration and the vertical velocity plots for these abscissa, while Fig. 7(d), Fig. 7(e) and Fig. 7(f) present the scaled plots

using the equations (16), (17) and (19).

- Fig. 8(a), Fig. 8(b) and Fig. 8(c) present the temperature, the concentration and the vertical velocity plots for the abscissa 2.0, 3.0 and 4.0 situated in the MDC_C region. Fig. 8(d), Fig. 8(e) and Fig. 8(f) show their scaled plots realised using the equations (33), (34) and (35).

- Similarly, Fig. 9(a), Fig. 9(b) and Fig. 9(c) present the temperature, the concentration and the vertical velocity plots for three abscissa: 6, 6.5 and 7 situated in the MDC_{Sc} region. Fig. 9(d), Fig. 9(e) and Fig. 9(f) show their scaled plots realised using the equations (28), (29) and (31). Fig. 7, Fig. 8 and Fig.9 verify the scale analysis results.

VI. CONCLUSIONS

This study reveals a set of conditions under which a vertical plane impermeable boundary situated in a constant temperature and mass stratified environment (air) determines the head and/or the mass driven convection regimes in the air adjacent to it. The boundary presents a constant temperature and the flux of a certain constituent is constant along the boundary.

The scale analysis reveals two situations that are encountered:

- $Ra \cdot S_C \cdot Sch^{4/3} / [N^3 Pr(1+Pr)] \geq 1$, where a HDC regime attains the equilibrium state.
- $Ra \cdot S_C \cdot Sch^{4/3} / [N^3 Pr(1+Pr)] < 1$, a HDC - MDC regimes succession attains the equilibrium state.

The finite differences method is used to solve the governing equations for two parameter sets in order to verify the scale analysis results.

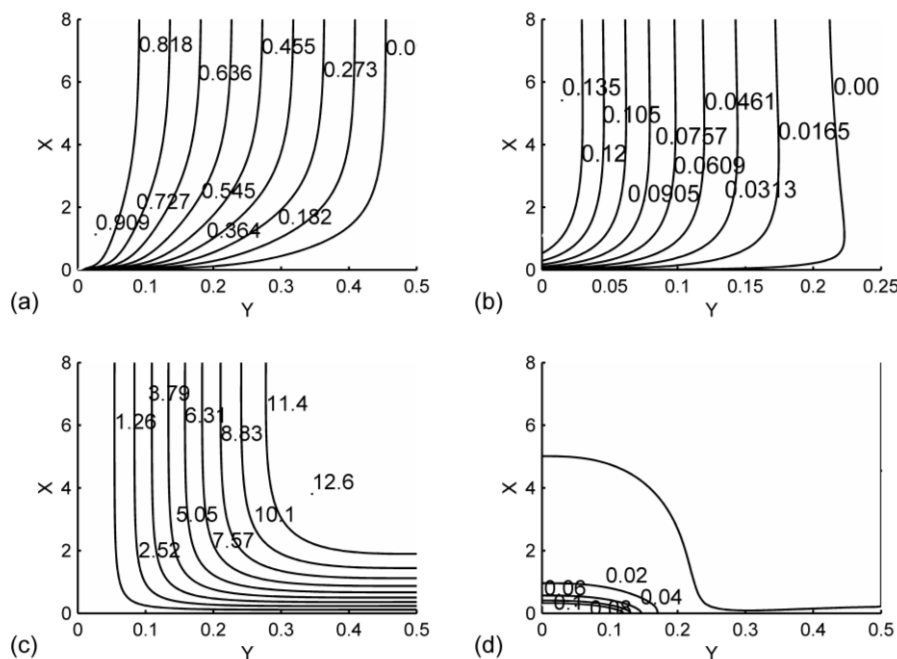


Fig. 6. The dimensionless temperature (a), concentration (b), stream function (c) and $\partial \phi / \partial x$ (d) fields. $Ra = 5000, N = 8, Le = 2, Pr = 0.72$ and $S_C = 0.04$.

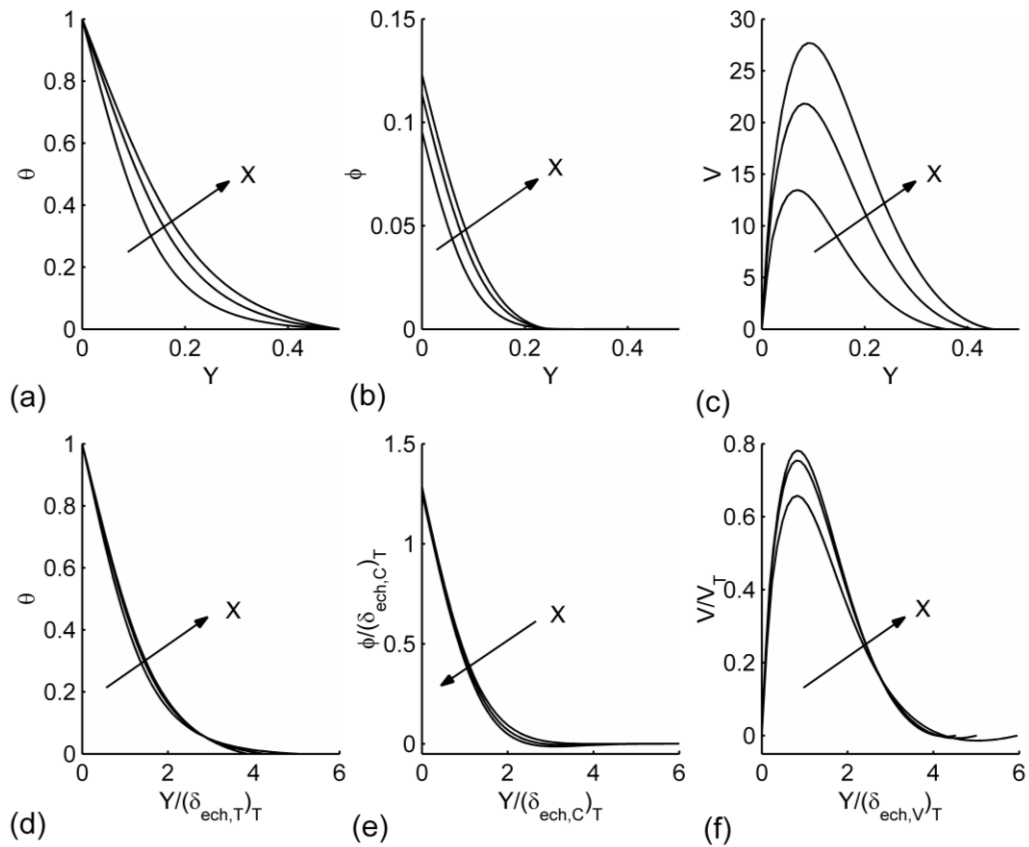


Fig. 7. The dimensionless (a) temperature, (b) concentration and (c) vertical velocity variations as a function of Y and the scaled (d) temperature, (e) concentration and (f) vertical velocity plots for the abscissas: 0.2, 0.4 and 0.6.

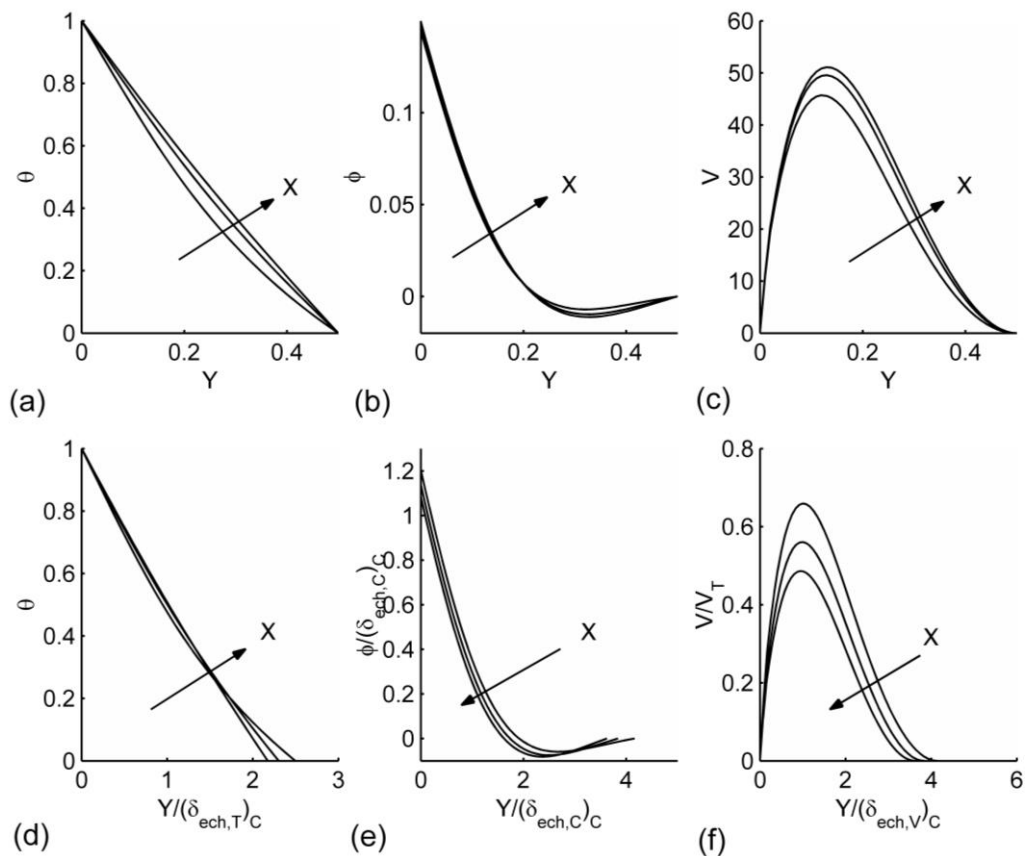


Fig. 8. The dimensionless (a) temperature, (b) concentration and (c) vertical velocity variations as a function of Y and the scaled (d) temperature, (e) concentration and (f) vertical velocity plots for the abscissas: 2.0, 3.0 and 4.0.

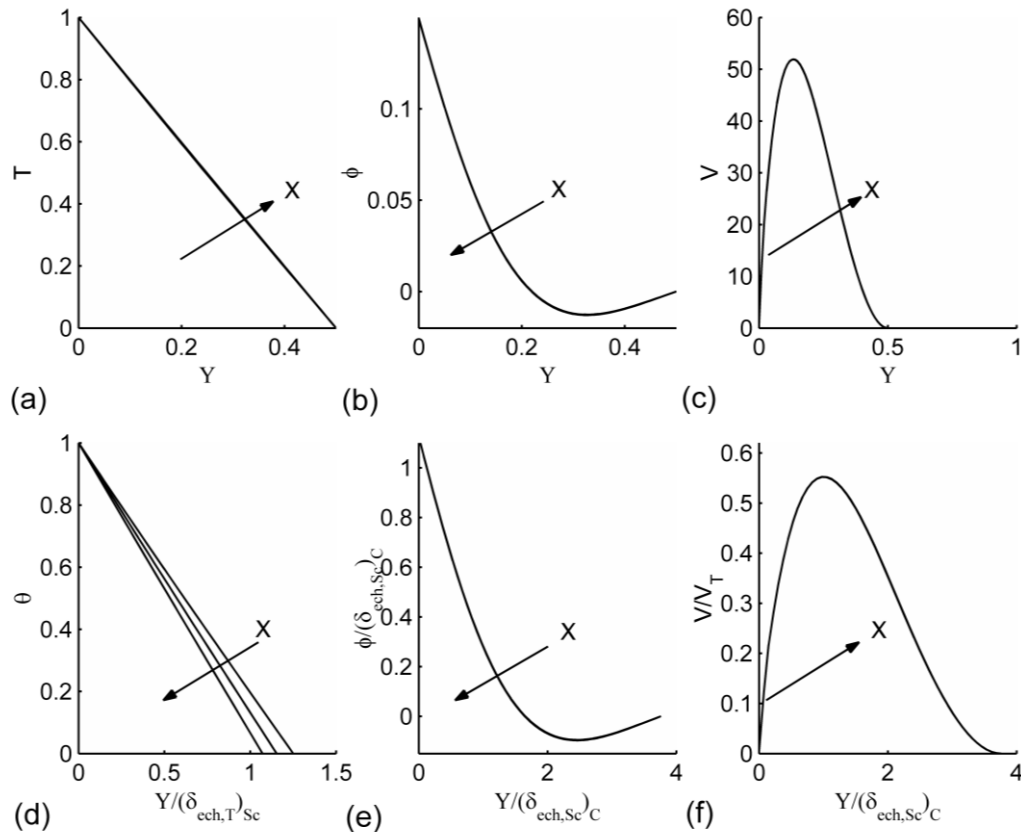


Fig. 9. The dimensionless (a) temperature, (b) concentration and (c) vertical velocity variations as a function of Y and the scaled (d) temperature, (e) concentration and (f) vertical velocity plots for the abscissas: 6.0, 6.5 and 7.0.

We can conclude that the HDC and/or the MDC regimes succession along a vertical impermeable wall is a characteristic of the natural convection process that takes place near a constant temperature and mass flux vertical impermeable boundary embedded in a mass stratified environment.

REFERENCES

[1] M. Neagu, "Free convection in a Darcy thermally stratified porous medium that embeds a vertical wall of constant heat flux and concentrations," World Academy of Science and Technology, International Journal of Mechanical, Aerospace, Industrial, Mechatronic and Manufacturing Engineering, vol. 10(1), 2016, pp. 65-74.

[2] M. Neagu, "Natural convection near a vertical wall of constant mass flux and temperature situated in a mass stratified fluid," IOP Conference Series: Materials Science and Engineering 444 0822020 doi: 10.1088/1757-899X/444/8/0822020, 2018, pp. 1-14.

[3] M. Neagu, "Natural convection in the boundary layer of a constant temperature and concentration vertical wall embedded in a Darcy doubly stratified porous medium," The Annals of "Dunarea de Jos" University of Galati, Fascicle V, 2017, pp. 13-20.

[4] M. Neagu, "Natural convection near a vertical wall of constant heat flux and concentration

embedded in a darcy mass stratified porous medium," The Annals of "Dunarea de Jos" University of Galati, Fascicle V, 2017, pp. 5-12.

[5] A. Bejan, "Convection heat transfer," second ed., John Wiley & Sons, Inc., New York, 1995, Chapter 4.

[6] S. C. Saha, J. C. Patterson and C. Lei, "Natural convection boundary-layer adjacent to an inclined flat plate subject to sudden and ramp heating," International Journal of Thermal Sciences, vol. 49, 2010, 1600-1612.

[7] S. W. Armfield, J. C. Patterson and W. Lin, "Scaling investigation of the natural convection boundary layer on an evenly heated plate," International Journal of heat and Mass Transfer, vol. 50, 2007, pp. 1592-1602.

[8] S. C. Saha, R. J. Brown and Y. T. Gu, "Scaling of the Prandtl number of the natural convection boundary layer of an inclined flat plate under uniform surface heat flux," International Journal of Heat and Mass Transfer, vol. 55, 2012, pp. 2394-2401.

[9] J. C. Tannehill, D. A. Anderson and R. H. Pletcher, "Computational fluid mechanics and heat transfer," second ed., Taylor&Francis, Washington, 1997, Chapter 3.